

Do the Amati and Yonetoku Relations Evolve with Redshift for *Swift* GRBs?

Ali M. Hasan, Walid J. Azzam

Department of Physics, College of Science, University of Bahrain, Sakhir, Bahrain

Email: wjazzam@uob.edu.bh, wjazzam@gmail.com

How to cite this paper: Hasan, A.M. and Azzam, W.J. (2026) Do the Amati and Yonetoku Relations Evolve with Redshift for *Swift* GRBs? *Journal of Applied Mathematics and Physics*, **14**, 1106-1119.
<https://doi.org/10.4236/jamp.2026.143052>

Received: February 12, 2026

Accepted: March 6, 2026

Published: March 9, 2026

Copyright © 2026 by author(s) and Scientific Research Publishing Inc.
This work is licensed under the Creative Commons Attribution International License (CC BY 4.0).
<http://creativecommons.org/licenses/by/4.0/>



Open Access

Abstract

Gamma-ray bursts (GRBs) are extremely powerful stellar explosions that have been observed to huge distances with redshifts exceeding 9. Although GRBs are not standard candles, one may “standardize” them by calibrating certain correlations that link an intrinsic parameter to an observed one. Two such correlations that have been discovered are the Amati relation and the Yonetoku relation. The former is a correlation between a burst’s equivalent isotropic energy, E_{iso} , and its intrinsic peak spectral energy $E_{p,b}$ while the latter is a correlation between a burst’s peak isotropic luminosity, L_{iso} , and $E_{p,i}$. In this paper, we compiled a large sample of 241 *Swift* long GRBs for the purpose of examining whether the Amati and Yonetoku relations are immune to redshift evolution. Our methodology encompasses two approaches: the first involves binning the data by redshift and fitting the two relations for each bin, then checking whether the fitting parameters evolve with redshift; the second approach involves using a redshift cutoff to divide the data into a low-redshift group and a high-redshift group, then checking whether the fitting parameters for the two relations are consistent with one another. Our results indicate that the Amati and Yonetoku relations are robust in the sense that they do not show any systematic or significant redshift evolution. Moreover, our results indicate that the high redshift bins show better fits compared to the low redshift bins, which indicates that the Amati and Yonetoku relations are more reliable as “standard candles” for high redshift and hence are promising cosmological probes.

Keywords

Gamma-Ray Bursts, Spectral Correlations, Redshift Evolution, Cosmological Probes

1. Introduction

Gamma-ray Bursts (GRBs) are extremely powerful explosions that have been ob-

served to very high redshift, which makes them particularly suitable for early universe investigations [1]-[3]. Although several studies have highlighted their potential as “standard candles” in cosmology [4]-[7], there are still a few enigmatic issues regarding their origins and properties. To resolve some of these issues, several studies examined the intrinsic characteristics of GRBs and found several important correlations among GRB parameters. One such correlation is the Amati relation, which links the equivalent isotropic energy E_{iso} of a burst to its intrinsic peak spectral energy $E_{p,i}$ through a power-law correlation, $E_{iso} \propto E_{p,i}^m$ [8]-[11]. As several studies stress, the Amati relation is important because it is a potential tool for constraining cosmological parameters [4] [5] [7] [12]-[16]. In addition, some studies argue that it can be used to classify GRBs. Traditionally, GRBs are classified into long GRBs (LGRBs) with $T_{90} > 2$ s and short GRBs (SGRBs) with $T_{90} < 2$ s, where T_{90} is the time taken to observe 90% of the GRB’s fluence [17]. However, this classification is not based on the intrinsic properties, making it prone to cosmological effects [18]-[22]. Recently, many studies have explored other methods of classification like employing the Amati relation as a discriminator among different GRB classes. More specifically, some recent studies have found evidence that SGRBs and LGRBs have different Amati slopes, which means that the Amati relation may be used to distinguish the two classes [23]-[25].

Another important correlation is the Yonetoku relation. The Yonetoku relation connects the peak isotropic luminosity L_{iso} to the intrinsic peak spectral energy $E_{p,i}$ through a power law as well, $L_{iso} \propto E_{p,i}^m$ [26]-[28]. Although some studies have utilized the Yonetoku relation as a distance indicator [7] [29], it is important to caution that to use the Yonetoku relation, or for that matter the Amati relation, as a cosmological probe, it must be calibrated properly. One problem that arises regarding the calibration of the Amati and Yonetoku relations is whether these correlations evolve with redshift. Both the Amati relation and the Yonetoku relation have been the subject of several studies that investigated their potential redshift evolution. Early studies found varying results regarding the evolution of these two relations [13] [28] [30]-[36]. For instance, a study in 2013 found evidence that the fitting slopes for both the Amati and Yonetoku relations do not evolve with redshift [37]. However, these studies suffered from the paucity of data points, as not many GRBs observed, at the time, had available redshift and spectral parameters.

As more input data have become available, there has been a revived interest in exploring whether intrinsic GRB correlations, like the Amati and Yonetoku relations, evolve with redshift. For instance, the recent study by Jia *et al.* [16], uses 221 GRBs to study the redshift evolution of the Amati relation. They split the dataset into 5 redshift bins and then fit each bin with the Amati relation. They find that the results of all the bins are consistent with one another within 2σ , suggesting no redshift evolution. On the other hand, two other studies, Singh *et al.* [38] and Singh *et al.* [39], find evidence of redshift evolution in the Amati relation. These two studies split their GRB datasets into low and high redshift subsets using a redshift cutoff and fit each data subset using the Amati relation. In [38], a redshift

cutoff of 1.5 is used for a GRB dataset composed of 162 bursts, and the authors find that their two subsets show an inconsistency in the Amati relation at the 2σ level, hinting at a possible redshift evolution. In the second study [39], the authors use the same dataset employed by [37] and carry out an analysis like that conducted by [38], and they find that again there is evidence, at the 2σ level, that the Amati relation evolves with redshift. On the other hand, less attention has been given in the past few years regarding the potential redshift evolution of the Yonetoku relation.

Given the importance of these two relations, we aim in this study to carry out a systematic investigation of their potential redshift evolution using a large dataset of 241 *Swift* LGRBs. In Section 2, we describe our data sample along with our methodology, and we present and discuss our results in Section 3. We provide a brief conclusion in Section 4.

2. Data Sample and Methodology

We compiled our GRB data sample from the *Swift* catalog [40]. As of July 2025, *Swift* has detected 1717 GRBs, of which 453 have reported redshifts. To fit the purpose of our study, we selected GRBs that satisfied the following criteria:

- The GRB must have a $T_{90} > 2$ s, in other words, it must be a long burst according to the traditional classification of GRBs [15] (27 GRBs removed).
- The GRB must have a single value detected redshift (12 GRBs removed).
- The GRB must have at least an estimated fluence S_{obs} , a 1-sec peak photon flux F_p , along with time-averaged and 1-sec peak spectral parameters. Note that in the catalog, only the power-law and the cutoff power-law fittings are reported and for our purpose, we use the latter as it provides an estimate of the peak energy E_p (153 GRBs removed).
- We excluded GRBs with large errors: exceeding 500% in their fluence, peak photon flux, or peak energy (20 GRBs removed).

This left us with 241 LGRBs suitable for our investigation. In addition, to account for the completeness of our dataset, we also compiled a subsample in which the bursts had a 1-sec peak photon flux $F_\gamma \geq 2.6$ photons/cm²/s. This new subset, which we will call the filtered dataset, has 87 LGRBs. For comparison reasons and to check the completeness of our original sample, we will report and compare the results of both datasets.

The redshift distribution of both datasets is shown in **Figure 1**. The redshift distribution of the unfiltered dataset is comparable to what we found in a previous study that we conducted [41], implying an excess of GRBs at low redshift compared to the star-formation rate [41]. Filtering the dataset by imposing the $F_\gamma \geq 2.6$ photons/cm²/s condition removes a substantial number of high redshift GRBs, leading to more excess GRBs at low redshift (when the distribution is normalized).

We wrote the Amati and Yonetoku relations in their logarithmic form and then carried out a linear fit:

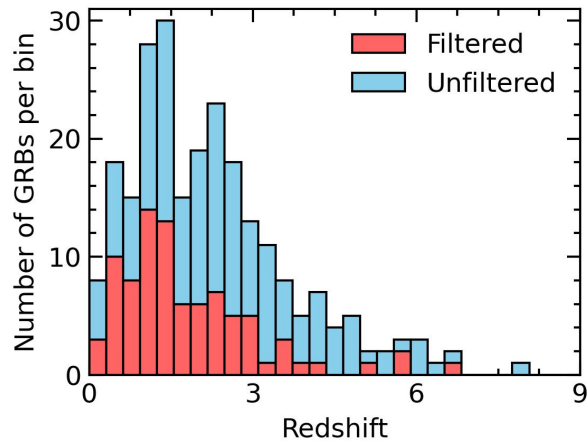


Figure 1. The redshift distribution of the datasets, with a bin size of 0.3.

$$\log\left(\frac{E_{iso}}{10^{52} \text{ erg}}\right) = A \log\left(\frac{E_{p,i}}{1 \text{ keV}}\right) + B, \tag{1}$$

$$\log\left(\frac{L_{iso}}{10^{52} \text{ erg/s}}\right) = A' \log\left(\frac{E_{p,i}}{1 \text{ keV}}\right) + B', \tag{2}$$

where $E_{p,i} = E_p^{obs} (1+z)$, is the intrinsic peak energy. E_{iso} and L_{iso} were calculated using the k -correction introduced by Bloom *et al.* (2001) [42] and implemented as detailed by Zitouni *et al.* (2014) [43]. Note that the *Swift* energy band is [15 - 150] keV and we considered the rest-frame energy band to be [1 - 10^4] keV for the k -correction method. For the cosmological parameters, we adopted the Λ CMD model with a Hubble constant $H_0 = 70.8 \text{ km/s/Mpc}$, $\Omega_M = 0.27$, and $\Omega_\Lambda = 1 - \Omega_M = 0.73$.

We employed two approaches to investigate the redshift evolution of the Amati and Yonetoku relations. First, a binning approach was used where the datasets were sorted according to redshift and then split into 3, 4 and 5 bins with an equal number of GRBs. Each bin was fitted individually with both relations. The second approach involved splitting the dataset into two groups, a low-redshift group and a high-redshift group, using a redshift cutoff. Each group was fitted with both relations. This method was used by Singh *et al.* [38] and Singh *et al.* [39], and following a similar procedure as the latter, we tried redshift cutoffs of 1.5 and 2.0 to split our datasets.

We used a least χ^2 method to find the best fit parameters, where χ^2 is calculated as follows:

$$\chi^2 = \sum_i \frac{\left(y_i^{obs} - y_i^{calc}\right)^2}{\sigma_{tot}^2}, \tag{3}$$

with $\sigma_{tot}^2 = \sigma_{obs}^2 + \sigma_{int}^2$. Here, σ_{int} is the intrinsic scattering parameter which encapsulates other errors not accounted for by the observational error. The optimization is run for parameters A, B and σ_{int} . In general, a smaller σ_{int} means that our model and the data fit well. This method is equivalent to maximizing the like-

likelihood function \mathcal{L} , which is related to χ^2 as follows:

$$\chi^2 = -2\ln(\mathcal{L}). \tag{4}$$

For all our fits, we report the fitting parameters, the intrinsic scattering parameter, and the Akaike Information Criterion (AIC). The AIC is calculated from the likelihood function \mathcal{L} or the χ^2 value in the following way [44] [45]:

$$\text{AIC} = 2k + \chi^2 = 2k - 2\ln(\mathcal{L}), \tag{5}$$

with k being the number of fitting parameters. Note that AIC is important when comparing datasets with different numbers of parameters, such as the binned datasets.

3. Results and Discussion

Table 1 provides a summary of calculated parameters and compares the unfiltered and filtered datasets. We note that the filtered dataset removes a good portion of low luminosity GRBs but also removes some high redshift GRBs, which are primarily high luminosity. This leads to a lower mean L_{iso} .

Table 1. A general description for the redshift, $E_{p,i}$, E_{iso} and L_{iso} for the unfiltered and filtered datasets.

Dataset		Redshift	$E_{p,i}$ (keV)	E_{iso} (ergs)	L_{iso} (ergs/s)
Unfiltered	Range	0.0389 - 8	16.56 - 4324.77	3.85×10^{48} - 6.04×10^{54}	1.36×10^{48} - 9.65×10^{55}
	Mean	2.23	439.95	2.91×10^{53}	5.01×10^{53}
Filtered	Range	0.13 - 6.782	37.53 - 3404.88	3.82×10^{50} - 6.04×10^{54}	1.08×10^{50} - 3.31×10^{54}
	Mean	1.81	496.95	4.01×10^{53}	1.65×10^{53}

Table 2. The Amati and Yonetoku fitting results for the unbinned datasets.

Relation	A	B	σ_{int}	AIC
Unfiltered dataset				
Amati	1.28 ± 0.15	-2.73 ± 0.36	0.82 ± 0.02	231.33
Yonetoku	2.24 ± 0.14	-5.69 ± 0.36	0.52 ± 0.01	172.26
Filtered dataset ($F_\gamma \geq 2.6$ photons/cm²/s)				
Amati	1.56 ± 0.22	-3.23 ± 0.57	0.70 ± 0.24	86.12
Yonetoku	2.20 ± 0.16	-5.32 ± 0.43	0.42 ± 0.03	74.41

Table 2 shows our Amati and Yonetoku fitting results for the unbinned datasets. We note that both datasets, the filtered and the unfiltered, are consistent with the Amati and Yonetoku relations, though the Yonetoku relation shows a better fit. Comparing the Amati parameters of the filtered and unfiltered datasets, we see that there is a difference between them, with the unfiltered results agreeing more with the results reported in [8], while the result of the filtered dataset is closer to that found by [39]. This then suggests that the Amati relation is prone to issues pertaining to the completeness of the dataset. As for the Yonetoku relation,

we find both datasets are consistent with each other, and they agree with the values reported in the literature [26].

Table 3. The Amati and Yonetoku fitting results for the binned unfiltered dataset.

Number of bins	Bin (redshift)	A	B	σ_{int}	AIC	Total AIC
Amati relation						
3 bins	Bin 1 (0.85 ± 0.36)	0.84 ± 0.35	-2.18 ± 0.81	0.98 ± 0.20	70.92	224.85
	Bin 2 (1.97 ± 0.36)	1.08 ± 0.20	-2.04 ± 0.50	0.70 ± 0.01	75.90	
	Bin 3 (3.89 ± 1.18)	0.87 ± 0.22	-1.40 ± 0.57	0.60 ± 0.13	74.03	
4 bins	Bin 1 (0.71 ± 0.30)	0.40 ± 0.43	-1.32 ± 0.99	1.06 ± 0.23	49.55	214.61
	Bin 2 (1.53 ± 0.24)	1.14 ± 0.30	-2.30 ± 0.75	0.76 ± 0.16	50.79	
	Bin 3 (2.44 ± 0.26)	1.05 ± 0.20	-1.98 ± 0.51	0.61 ± 0.01	56.63	
	Bin 4 (4.27 ± 1.12)	0.89 ± 0.26	-1.40 ± 0.69	0.62 ± 0.14	57.64	
5 bins	Bin 1 (0.62 ± 0.26)	0.39 ± 0.52	-1.46 ± 1.17	1.12 ± 0.28	34.65	221.24
	Bin 2 (1.30 ± 0.15)	0.70 ± 0.30	-1.32 ± 0.74	0.75 ± 0.57	43.99	
	Bin 3 (1.98 ± 0.24)	2.13 ± 0.28	-4.61 ± 0.72	0.55 ± 0.02	46.73	
	Bin 4 (2.74 ± 0.26)	0.75 ± 0.19	-1.22 ± 0.49	0.57 ± 0.17	49.17	
	Bin 5 (4.56 ± 1.07)	0.89 ± 0.32	-1.38 ± 0.86	0.63 ± 0.15	46.70	
Yonetoku relation						
3 bins	Bin 1 (0.85 ± 0.36)	1.54 ± 0.34	-4.35 ± 0.82	0.67 ± 0.06	65.76	163.96
	Bin 2 (1.97 ± 0.36)	2.06 ± 0.18	-5.07 ± 0.49	0.34 ± 0.01	52.14	
	Bin 3 (3.89 ± 1.18)	1.88 ± 0.19	-4.41 ± 0.53	0.23 ± 0.01	46.06	
4 bins	Bin 1 (0.71 ± 0.30)	1.15 ± 0.40	-3.55 ± 0.96	0.71 ± 0.16	49.17	167.60
	Bin 2 (1.53 ± 0.24)	1.93 ± 0.23	-4.83 ± 0.59	0.33 ± 0.01	46.32	
	Bin 3 (2.44 ± 0.26)	1.99 ± 0.21	-4.72 ± 0.58	0.30 ± 0.01	38.49	
	Bin 4 (4.27 ± 1.12)	2.25 ± 0.16	-5.53 ± 0.49	0.00 ± 0.00	33.62	
5 bins	Bin 1 (0.62 ± 0.26)	1.10 ± 0.46	-3.52 ± 1.09	0.77 ± 0.30	37.92	165.35
	Bin 2 (1.30 ± 0.15)	1.86 ± 0.25	-4.77 ± 0.66	0.37 ± 0.01	36.76	
	Bin 3 (1.98 ± 0.24)	2.24 ± 0.25	-5.49 ± 0.67	0.36 ± 0.03	34.52	
	Bin 4 (2.74 ± 0.26)	1.72 ± 0.25	-3.98 ± 0.69	0.28 ± 0.02	28.77	
	Bin 5 (4.56 ± 1.07)	2.27 ± 0.18	-5.59 ± 0.54	0.00 ± 0.00	27.39	

Our results for the unfiltered and filtered binned datasets are presented in **Table 3** and **Table 4**, respectively. A visual comparison between the parameters is shown in **Figure 2** and **Figure 3**, for the unfiltered and filtered dataset, respectively. For the Amati relation, we see that the unfiltered dataset shows no redshift evolution, with all the bins being within at most 2σ from each other and from the full dataset fitting parameters. The filtered dataset shows a trend when moving from low to high redshift, especially for 5 bins, where the high redshift bins show strong agreement with the fitting of the whole dataset. But one cannot claim there is a redshift

evolution here due to the large errors where all the bins are within a 1σ range. The different behavior between the two datasets further suggests that the Amati relation is affected by the completeness of the dataset. Overall, the Amati relation does not show clear signs of redshift evolution. The Yonetoku relation, in a similar manner, does not show any redshift evolution behavior with all bins being within 2σ . However, the high redshift bins appear to be more consistent and show better fitting than low redshift ones, which is witnessed by comparing them to the whole dataset parameters and is also reflected in the σ_{int} trends. In both datasets, the σ_{int} value in the high redshift bins is smaller than the low redshift bins, suggesting that it fits the model better. In other words, the Yonetoku relation is more reliable for high redshift GRBs than for low redshift ones.

Table 4. The Amati and Yonetoku fitting results for the binned filtered dataset.

Number of bins	Bin (redshift)	A	B	σ_{int}	AIC	Total AIC
Amati relation						
3 bins	Bin 1 (0.85 ± 0.36)	0.56 ± 0.53	-1.25 ± 1.20	0.67 ± 2.18	31.59	84.37
	Bin 2 (1.97 ± 0.36)	1.35 ± 0.57	-2.53 ± 1.47	0.89 ± 0.51	23.77	
	Bin 3 (3.89 ± 1.18)	1.25 ± 0.31	-2.20 ± 0.86	0.49 ± 0.16	29.00	
4 bins	Bin 1 (0.71 ± 0.30)	0.51 ± 0.67	-1.24 ± 1.54	0.70 ± 0.26	18.56	81.58
	Bin 2 (1.53 ± 0.24)	0.46 ± 0.46	-0.66 ± 1.14	0.70 ± 0.37	23.70	
	Bin 3 (2.44 ± 0.26)	1.89 ± 0.39	-3.70 ± 1.06	0.52 ± 0.12	20.80	
	Bin 4 (4.27 ± 1.12)	1.00 ± 0.47	-1.53 ± 1.32	0.62 ± 0.31	18.51	
5 bins	Bin 1 (0.62 ± 0.26)	0.09 ± 0.80	-0.40 ± 1.81	0.77 ± 0.31	13.25	85.41
	Bin 2 (1.30 ± 0.15)	0.61 ± 0.64	-1.07 ± 1.54	0.61 ± 0.24	21.46	
	Bin 3 (1.98 ± 0.24)	0.81 ± 0.58	-1.18 ± 1.49	0.78 ± 0.35	17.89	
	Bin 4 (2.74 ± 0.26)	1.32 ± 0.39	-2.25 ± 1.08	0.52 ± 0.15	18.82	
	Bin 5 (4.56 ± 1.07)	1.48 ± 0.67	-2.84 ± 1.88	0.69 ± 0.34	14.00	
Yonetoku relation						
3 bins	Bin 1 (0.85 ± 0.36)	0.95 ± 0.47	-2.73 ± 1.10	0.48 ± 0.10	25.75	72.85
	Bin 2 (1.97 ± 0.36)	2.09 ± 0.24	-4.96 ± 0.65	0.28 ± 0.03	26.56	
	Bin 3 (3.89 ± 1.18)	1.65 ± 0.18	-3.50 ± 0.52	0.16 ± 0.01	20.54	
4 bins	Bin 1 (0.71 ± 0.30)	1.16 ± 0.69	-3.33 ± 1.60	0.54 ± 0.19	18.61	74.63
	Bin 2 (1.53 ± 0.24)	1.65 ± 0.22	-3.96 ± 0.57	0.23 ± 0.02	18.77	
	Bin 3 (2.44 ± 0.26)	2.10 ± 0.26	-4.86 ± 0.73	0.27 ± 0.04	21.42	
	Bin 4 (4.27 ± 1.12)	1.58 ± 0.25	-3.28 ± 0.71	0.15 ± 0.01	15.82	
5 bins	Bin 1 (0.62 ± 0.26)	0.76 ± 0.77	-2.56 ± 1.79	0.54 ± 0.20	13.16	76.98
	Bin 2 (1.30 ± 0.15)	0.86 ± 0.32	-2.13 ± 0.79	0.15 ± 0.03	16.77	
	Bin 3 (1.98 ± 0.24)	1.84 ± 0.24	-4.32 ± 0.63	0.18 ± 0.02	15.62	
	Bin 4 (2.74 ± 0.26)	1.82 ± 0.22	-3.92 ± 0.63	0.20 ± 0.06	19.27	
	Bin 5 (4.56 ± 1.07)	1.76 ± 0.27	-3.87 ± 0.84	0.00 ± 0.00	12.16	

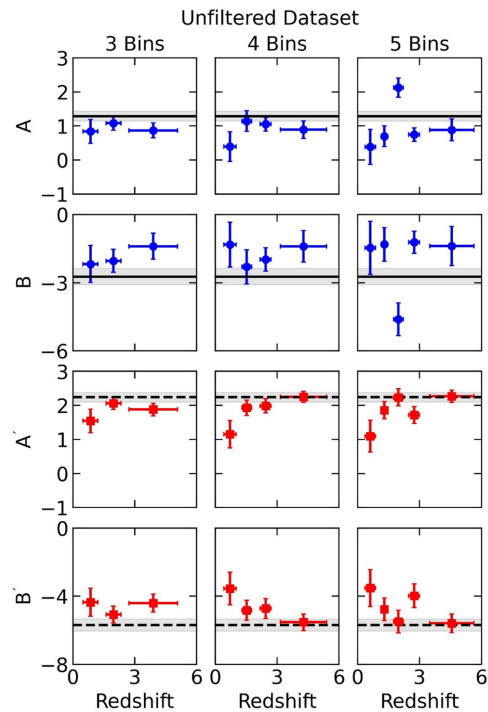


Figure 2. The fitting results for the binned unfiltered dataset shown for 3, 4, and 5 bins. The values for the fitting parameters, A and B, for the Amati and Yonetoku relations are shown in blue and red, respectively. For comparison, the horizontal lines, solid and dashed, show the values of A and B when the entire unfiltered dataset is used (*i.e.*, without binning).

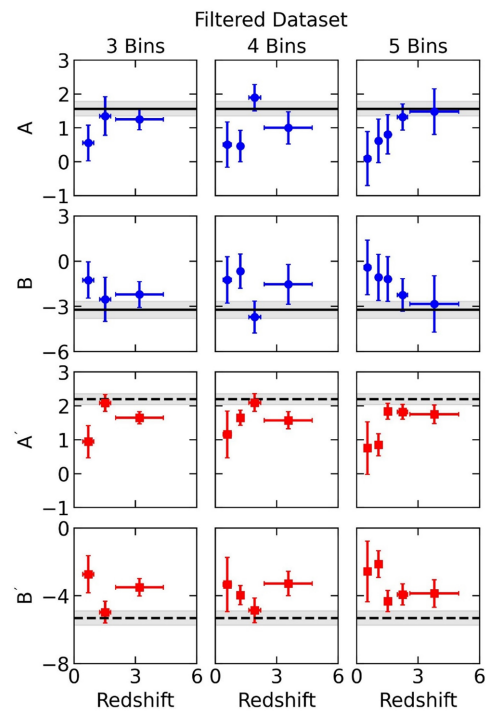


Figure 3. The fitting results for the binned filtered dataset shown for 3, 4, and 5 bins. The values for the fitting parameters, A and B, for the Amati and Yonetoku relations are shown in blue and red, respectively. For comparison, the horizontal lines, solid and dashed, show the values of A and B when the entire filtered dataset is used (*i.e.*, without binning).

Table 5 presents our results for the cutoff splitting of both datasets. We can see that the results from both datasets agree with the parameters found from fitting the whole datasets (**Table 2**), within at most 2σ . Again, we find that the high redshift groups, $z \geq z_{\text{cutoff}}$, show better fits and are closer to the whole dataset fitting than the low redshift groups, $z < z_{\text{cutoff}}$ groups.

Table 5. The Amati and Yonetoku relations fitting results for the datasets that were split into groups using a redshift cutoff.

Relation	Group	A	B	σ_{int}	AIC	Total AIC
Unfiltered dataset						
Cutoff $z_{\text{cutoff}} = 1.5$						
Amati	$z < 1.5$ (94 GRB)	0.81 ± 0.29	-2.03 ± 0.67	0.95 ± 0.18	86.14	225.76
	$z \geq 1.5$ (147 GRB)	1.13 ± 0.15	-2.09 ± 0.38	0.62 ± 0.01	139.62	
Yonetoku	$z < 1.5$ (94 GRB)	1.76 ± 0.28	-4.81 ± 0.67	0.65 ± 0.03	74.42	161.34
	$z \geq 1.5$ (147 GRB)	2.05 ± 0.14	-4.97 ± 0.39	0.30 ± 0.01	86.92	
Cutoff $z_{\text{cutoff}} = 2$						
Amati	$z < 2$ (122 GRB)	1.11 ± 0.25	-2.58 ± 0.61	0.94 ± 0.13	112.58	227.88
	$z \geq 2$ (119 GRB)	1.04 ± 0.15	-1.87 ± 0.40	0.60 ± 0.01	115.30	
Yonetoku	$z < 2$ (122 GRB)	1.89 ± 0.23	-5.01 ± 0.57	0.61 ± 0.02	98.55	166.54
	$z \geq 2$ (119 GRB)	2.04 ± 0.14	-4.87 ± 0.41	0.24 ± 0.01	67.99	
Filtered dataset ($F_{\gamma} \geq 2.6 \text{ erg/cm}^2/\text{s}$)						
Cutoff $z_{\text{cutoff}} = 1.5$						
Amati	$z < 1.5$ (45 GRB)	0.74 ± 0.34	-1.54 ± 0.81	0.65 ± 0.29	48.37	86.72
	$z \geq 1.5$ (42 GRB)	1.39 ± 0.31	-2.48 ± 0.84	0.58 ± 0.13	38.35	
Yonetoku	$z < 1.5$ (45 GRB)	1.74 ± 0.28	-4.41 ± 0.67	0.44 ± 0.05	39.66	73.58
	$z \geq 1.5$ (42 GRB)	1.90 ± 0.18	-4.27 ± 0.51	0.23 ± 0.02	33.92	
Cutoff $z_{\text{cutoff}} = 2$						
Amati	$z < 2$ (56 GRB)	1.20 ± 0.35	-2.48 ± 0.84	0.74 ± 0.27	56.27	86.47
	$z \geq 2$ (31 GRB)	1.33 ± 0.33	-2.38 ± 0.94	0.55 ± 0.21	30.20	
Yonetoku	$z < 2$ (56 GRB)	1.82 ± 0.26	-4.78 ± 0.65	0.45 ± 0.05	50.50	73.02
	$z \geq 2$ (31 GRB)	1.69 ± 0.17	-3.60 ± 0.51	0.16 ± 0.01	22.52	

In summary, high redshift bins always show better fitting than low redshift ones, regardless of the splitting method used, as noted from the σ_{int} and AIC values. This indicates that both relations are more reliable for high redshift *Swift* GRBs than for low redshift ones. The large σ_{int} and errors in the fitted parameters, A and B, of the Amati relation at low redshift suggest that the observational error does not encapsulate all the errors in the data. There is either an underestimation of the error or potentially new interesting physics at low redshift. The Yonetoku relation does not suffer from such problems. Additionally, the Yonetoku relation

shows more consistent results for the two different datasets and is thus more reliable according to our results.

Since our results indicate that the Amati and Yonetoku relations are less reliable for the low redshift *Swift* LGRBs compared to the high redshift bursts, one might, for better accuracy and more targeted applications, exclusively use high redshift LGRBs to get better fits. The aim of the Amati and Yonetoku relations is to investigate the early universe, hence focusing on high redshift GRBs can cater more to this application of the two relations. We also note that in this case, the condition $F_\gamma \geq 2.6$ photons/cm²/s, is not sufficient by itself, as many high redshift GRBs were eliminated, which affects the high redshift fittings. For better high-redshift investigations, one should account for the truncation of the dataset by methods such as the Efron-Petrosian method [46].

The question remains as to why we get relatively poorer fits from low redshift GRBs. One reason could be due to different origins of observed low redshift GRBs. As previously mentioned, it has been reported that there is an observed low redshift excess of LGRBs when one compares the redshift distribution of GRBs to the star-formation rate [41] [47]-[50]. Recent studies suggest that these LGRBs may emanate from other sources, like compact object mergers [48] [51]-[53], in which case the difference that we report regarding the applicability of the Amati and Yonetoku relations for low and high redshift might not be surprising.

4. Conclusion

In this work, the redshift evolution of the Amati and Yonetoku relations was investigated using *Swift* GRBs. A dataset of 241 LGRBs was compiled to carry out the investigation. In addition, a smaller subset of 87 LGRBs was formed that satisfied the condition $F_\gamma \geq 2.6$ photons/cm²/s. Both datasets showed better fitting for the Yonetoku relation compared to the Amati relation. Two approaches were used to assess the redshift evolution of the two relations, the first one being a binning method where the datasets were split into 3, 4 and 5 equal bins and fit accordingly, and the second one was a redshift cutoff based split. Both approaches showed consistent results, with no clear redshift evolution being observed. However, our results indicate that the low redshift bins show poorer fits compared to the high redshift bins, thus making the Amati and Yonetoku relations more reliable for high redshift bursts and hence suitable for cosmological investigations.

Conflicts of Interest

The authors declare no conflicts of interest regarding the publication of this paper.

References

- [1] Klebesadel, R.W., Strong, I.B. and Olson, R.A. (1973) Observations of Gamma-Ray Bursts of Cosmic Origin. *The Astrophysical Journal*, **182**, L85-L88. <https://doi.org/10.1086/181225>
- [2] Tanvir, N., Fox, D., Levan, A., *et al.* (2009) A γ Ray Burst at a Redshift of $Z \approx 8.2$.

- Nature*, **461**, 1254-1257.
- [3] Salvaterra, R., Valle, M.D., Campana, S., Chincarini, G., Covino, S., D'Avanzo, P., *et al.* (2009) GRB 090423 at a Redshift of $Z \approx 8.1$. *Nature*, **461**, 1258-1260. <https://doi.org/10.1038/nature08445>
- [4] Dainotti, M.G., Lenart, A.L., Chraya, A., Sarracino, G., Nagataki, S., Fraija, N., *et al.* (2022) The Gamma-Ray Bursts Fundamental Plane Correlation as a Cosmological Tool. *Monthly Notices of the Royal Astronomical Society*, **518**, 2201-2240. <https://doi.org/10.1093/mnras/stac2752>
- [5] Kumar, D., Rani, N., Jain, D., Mahajan, S. and Mukherjee, A. (2023) Gamma Rays Bursts: A Viable Cosmological Probe? *Journal of Cosmology and Astroparticle Physics*, **2023**, Article No. 021. <https://doi.org/10.1088/1475-7516/2023/07/021>
- [6] Horvath, I., Bagoly, Z., Balazs, L.G., Hakkila, J., Horvath, Z., Joo, A.P., *et al.* (2023) Mapping the Universe with Gamma-Ray Bursts. *Monthly Notices of the Royal Astronomical Society*, **527**, 7191-7202. <https://doi.org/10.1093/mnras/stad3669>
- [7] Bargiacchi, G., Dainotti, M.G. and Capozziello, S. (2025) High-Redshift Cosmology by Gamma-Ray Bursts: An Overview. *New Astronomy Reviews*, **100**, Article 101712. <https://doi.org/10.1016/j.newar.2024.101712>
- [8] Amati, L., Frontera, F., Tavani, M., in 't Zand, J.J.M., Antonelli, A., Costa, E., *et al.* (2002) Intrinsic Spectra and Energetics of BeppoSax Gamma-Ray Bursts with Known Redshifts. *Astronomy & Astrophysics*, **390**, 81-89. <https://doi.org/10.1051/0004-6361:20020722>
- [9] Amati, L. (2006) The $E_{p,i}-E_{iso}$ Correlation in Gamma-Ray Bursts: Updated Observational Status, Re-Analysis and Main Implications. *Monthly Notices of the Royal Astronomical Society*, **372**, 233-245. <https://doi.org/10.1111/j.1365-2966.2006.10840.x>
- [10] Amati, L., Guidorzi, C., Frontera, F., Della Valle, M., Finelli, F., Landi, R., *et al.* (2008) Measuring the Cosmological Parameters with the $E_{p,i}-E_{iso}$ Correlation of Gamma-Ray Bursts. *Monthly Notices of the Royal Astronomical Society*, **391**, 577-584. <https://doi.org/10.1111/j.1365-2966.2008.13943.x>
- [11] Amati, L., Frontera, F. and Guidorzi, C. (2009) Extremely Energetic *Fermi* Gamma-Ray Bursts Obey Spectral Energy Correlations. *Astronomy & Astrophysics*, **508**, 173-180. <https://doi.org/10.1051/0004-6361/200912788>
- [12] Amati, L. (2012) Cosmology with the $E_{p,i}-E_{iso}$ Correlation of Gamma-Ray Bursts. *International Journal of Modern Physics: Conference Series*, **12**, 19-27. <https://doi.org/10.1142/s2010194512006228>
- [13] Amati, L. and Valle, M.D. (2013) Measuring Cosmological Parameters with Gamma Ray Bursts. *International Journal of Modern Physics D*, **22**, Article 1330028. <https://doi.org/10.1142/s0218271813300280>
- [14] Azzam, W.J. (2016) A Brief Review of the Amati Relation for GRBs. *International Journal of Astronomy and Astrophysics*, **6**, 378-383. <https://doi.org/10.4236/ijaa.2016.64030>
- [15] Demianski, M., Piedipalumbo, E., Sawant, D. and Amati, L. (2017) Cosmology with Gamma-Ray Bursts: I. The Hubble Diagram through the Calibrated $E_{p,i}-E_{iso}$ Correlation. *Astronomy & Astrophysics*, **598**, A112. <https://doi.org/10.1051/0004-6361/201628909>
- [16] Jia, X.D., Hu, J.P., Yang, J., Zhang, B.B. and Wang, F.Y. (2022) $E_{iso}-E_p$ Correlation of Gamma-Ray Bursts: Calibration and Cosmological Applications. *Monthly Notices of the Royal Astronomical Society*, **516**, 2575-2585.

- <https://doi.org/10.1093/mnras/stac2356>
- [17] Kouveliotou, C., Meegan, C.A., Fishman, G.J., Bhat, N.P., Briggs, M.S., Koshut, T.M., *et al.* (1993) Identification of Two Classes of Gamma-Ray Bursts. *The Astrophysical Journal*, **413**, L101. <https://doi.org/10.1086/186969>
- [18] Zitouni, H., Guessoum, N., Azzam, W.J. and Mochkovitch, R. (2015) Statistical Study of Observed and Intrinsic Durations among BATSE and Swift/Bat GRBs. *Astrophysics and Space Science*, **357**, Article No. 7. <https://doi.org/10.1007/s10509-015-2311-x>
- [19] Ruffini, R., Rueda, J.A., Muccino, M., Aimuratov, Y., Becerra, L.M., Bianco, C.L., *et al.* (2016) On the Classification of GRBs and Their Occurrence Rates. *The Astrophysical Journal*, **832**, Article No. 136. <https://doi.org/10.3847/0004-637x/832/2/136>
- [20] Tarnopolski, M. (2016) Analysis of the Observed and Intrinsic Durations of Gamma-Ray Bursts with Known Redshift. *Astrophysics and Space Science*, **361**, Article No. 125. <https://doi.org/10.1007/s10509-016-2687-2>
- [21] Salmon, L., Hanlon, L. and Martin-Carrillo, A. (2022) Two Classes of Gamma-Ray Bursts Distinguished within the First Second of Their Prompt Emission. *Galaxies*, **10**, Article No. 78. <https://doi.org/10.3390/galaxies10040078>
- [22] Steinhardt, C.L., Mann, W.J., Rusakov, V. and Jespersen, C.K. (2023) Classification of BATSE, Swift, and Fermi Gamma-Ray Bursts from Prompt Emission Alone. *The Astrophysical Journal*, **945**, Article No. 67. <https://doi.org/10.3847/1538-4357/acb999>
- [23] Azzam, W.J., Jaber, F.S. and Ahmed, G.M. (2022) The $E_{\text{iso}}-L_{\text{iso}}$ Plane for Gamma Ray Bursts. *Journal of Applied Mathematics and Physics*, **10**, 1083-1088. <https://doi.org/10.4236/jamp.2022.104074>
- [24] Azzam, W.J., Jaber, F.S. and Naeem, A. (2020) An Amati-Like Correlation for Short Gamma-Ray Bursts. *Journal of Applied Mathematics and Physics*, **8**, 2371-2378. <https://doi.org/10.4236/jamp.2020.811175>
- [25] Zitouni, H., Guessoum, N. and Azzam, W. (2022) Testing the Amati and Yonetoku Correlations for Short Gamma-Ray Bursts. *Astrophysics and Space Science*, **367**, Article No. 74. <https://doi.org/10.1007/s10509-022-04100-2>
- [26] Yonetoku, D., Murakami, T., Nakamura, T., Yamazaki, R., Inoue, A.K. and Ioka, K. (2004) Gamma-Ray Burst Formation Rate Inferred from the Spectral Peak Energy-Peak Luminosity Relation. *The Astrophysical Journal*, **609**, 935-951. <https://doi.org/10.1086/421285>
- [27] Ghirlanda, G., Nava, L. and Ghisellini, G. (2010) Spectral-Luminosity Relation within Individual *Fermi* Gamma Rays Bursts. *Astronomy and Astrophysics*, **511**, A43. <https://doi.org/10.1051/0004-6361/200913134>
- [28] Yonetoku, D., Murakami, T., Tsutsui, R., Nakamura, T., Morihara, Y. and Takahashi, K. (2010) Possible Origins of Dispersion of the Peak Energy-Brightness Correlations of Gamma-Ray Bursts. *Publications of the Astronomical Society of Japan*, **62**, 1495-1507. <https://doi.org/10.1093/pasj/62.6.1495>
- [29] Aldowma, T. and Razzaque, S. (2024) Deep Neural Networks for Estimation of Gamma-Ray Burst Redshifts. *Monthly Notices of the Royal Astronomical Society*, **529**, 2676-2685. <https://doi.org/10.1093/mnras/stae535>
- [30] Band, D.L. and Preece, R.D. (2005) Testing the Gamma-Ray Burst Energy Relationships. *The Astrophysical Journal*, **627**, 319-323. <https://doi.org/10.1086/430402>
- [31] Nakar, E. and Piran, T. (2005) Outliers to the Peak Energy-Isotropic Energy Relation in Gamma-Ray Bursts. *Monthly Notices of the Royal Astronomical Society: Letters*, **360**, L73-L76. <https://doi.org/10.1111/j.1745-3933.2005.00049.x>
- [32] Ghirlanda, G., Ghisellini, G. and Firmani, C. (2005) Probing the Existence of the $E_{\text{peak}}-E_{\text{iso}}$ Correlation in Long Gamma Ray Bursts. *Monthly Notices of the Royal Astro-*

- nomical Society: Letters*, **361**, L10-L14.
<https://doi.org/10.1111/j.1745-3933.2005.00053.x>
- [33] Ghirlanda, G., Nava, L., Ghisellini, G., Firmani, C. and Cabrera, J.I. (2008) The $E_{\text{peak}}-E_{\text{iso}}$ Plane of Long Gamma-Ray Bursts and Selection Effects. *Monthly Notices of the Royal Astronomical Society*, **387**, 319-330.
<https://doi.org/10.1111/j.1365-2966.2008.13232.x>
- [34] Collazzi, A.C., Schaefer, B.E., Goldstein, A. and Preece, R.D. (2012) A Significant Problem with Using the Amati Relation for Cosmological Purposes. *The Astrophysical Journal*, **747**, Article 39. <https://doi.org/10.1088/0004-637x/747/1/39>
- [35] Heussaff, V., Atteia, J.-L. and Zolnierowski, Y. (2013) The $E_{\text{peak}}-E_{\text{iso}}$ Relation Revisited with *Fermi* GRBs. *Astronomy & Astrophysics*, **557**, A100.
<https://doi.org/10.1051/0004-6361/201321528>
- [36] Shahmoradi, A. (2013) A Multivariate Fit Luminosity Function and World Model for Long Gamma-Ray Bursts. *The Astrophysical Journal*, **766**, Article 111.
<https://doi.org/10.1088/0004-637x/766/2/111>
- [37] Azzam, W.J. and Alothman, M.J. (2013) Redshift Independence of the Amati and Yonetoku Relations for Gamma-Ray Bursts. *International Journal of Astronomy and Astrophysics*, **3**, 372-375. <https://doi.org/10.4236/ijaa.2013.34042>
- [38] Singh, M., Singh, D., Lal Pandey, K., Verma, D. and Gupta, S. (2024) Investigating the Evolution of Amati Parameters with Redshift. *Research in Astronomy and Astrophysics*, **24**, Article 015015. <https://doi.org/10.1088/1674-4527/ad0fd5>
- [39] Singh, D., Singh, M., Verma, D., Pandey, K.L. and Gupta, S. (2025) Does the Amati Correlation Exhibit Redshift-Driven Heterogeneity in Long GRBs? *Physics Letters B*, **866**, Article 139500. <https://doi.org/10.1016/j.physletb.2025.139500>
- [40] (2025) Swift Results Page. <https://swift.gsfc.nasa.gov/results/>
- [41] Hasan, A.M. and Azzam, W.J. (2024) Does the Redshift Distribution of Swift Long GRBs Trace the Star-Formation Rate? *International Journal of Astronomy and Astrophysics*, **14**, 20-44. <https://doi.org/10.4236/ijaa.2024.141002>
- [42] Bloom, J.S., Frail, D.A. and Sari, R. (2001) The Prompt Energy Release of Gamma-Ray Bursts Using a Cosmological K -Correction. *The Astronomical Journal*, **121**, 2879-2888.
<https://doi.org/10.1086/321093>
- [43] Zitouni, H., Guessoum, N. and Azzam, W.J. (2014) Revisiting the Amati and Yonetoku Correlations with Swift GRBs. *Astrophysics and Space Science*, **351**, 267-279.
<https://doi.org/10.1007/s10509-014-1839-5>
- [44] Akaike, H. (1974) A New Look at the Statistical Model Identification. *IEEE Transactions on Automatic Control*, **19**, 716-723. <https://doi.org/10.1109/tac.1974.1100705>
- [45] Liddle, A.R. (2007) Information Criteria for Astrophysical Model Selection. *Monthly Notices of the Royal Astronomical Society: Letters*, **377**, L74-L78.
<https://doi.org/10.1111/j.1745-3933.2007.00306.x>
- [46] Efron, B. and Petrosian, V. (1992) A Simple Test of Independence for Truncated Data with Applications to Redshift Surveys. *The Astrophysical Journal*, **399**, 345-352.
<https://doi.org/10.1086/171931>
- [47] Dong, X.F., Li, X.J., Zhang, Z.B. and Zhang, X.L. (2022) A Comparative Study of Luminosity Functions and Event Rate Densities of Long GRBs with Non-Parametric Method. *Monthly Notices of the Royal Astronomical Society*, **513**, 1078-1087.
<https://doi.org/10.1093/mnras/stac949>
- [48] Dong, X.F., Zhang, Z.B., Li, Q.M., Huang, Y.F. and Bian, K. (2023) The Origin of Low-Redshift Event Rate Excess as Revealed by the Low-Luminosity Gamma-Ray

- Bursts. *The Astrophysical Journal*, **958**, Article No. 37.
<https://doi.org/10.3847/1538-4357/acf852>
- [49] Liu, Y., Zhang, Z.B., Dong, X.F., Li, L.B. and Du, X.Y. (2025) The Event Rate and Luminosity Function of *Fermi*/GBM Gamma-Ray Bursts. *Monthly Notices of the Royal Astronomical Society*, **542**, 215-222. <https://doi.org/10.1093/mnras/staf1217>
- [50] Dong, X., Huang, Y., Zhang, Z., Geng, J., Deng, C., Zou, Z., *et al.* (2025) A Statistical Study of the Gamma-Ray Burst and Supernova Association. *The Astrophysical Journal*, **993**, Article 20. <https://doi.org/10.3847/1538-4357/ae04e7>
- [51] Troja, E., Fryer, C.L., O'Connor, B., Ryan, G., Dichiara, S., Kumar, A., *et al.* (2022) A Nearby Long Gamma-Ray Burst from a Merger of Compact Objects. *Nature*, **612**, 228-231. <https://doi.org/10.1038/s41586-022-05327-3>
- [52] Petrosian, V. and Dainotti, M.G. (2024) Progenitors of Low-Redshift Gamma-Ray Bursts. *The Astrophysical Journal Letters*, **963**, L12.
<https://doi.org/10.3847/2041-8213/ad2763>
- [53] Lloyd-Ronning, N.M., Johnson, J., Upton Sanderbeck, P., Silva, M. and Cheng, R.M. (2024) White Dwarf-Black Hole Binary Progenitors of Low-Redshift Gamma-Ray Bursts. *Monthly Notices of the Royal Astronomical Society*, **535**, 2800-2811.
<https://doi.org/10.1093/mnras/stae2502>